Available online at www.sciencedirect.com

SciVerse ScienceDirect

Ceramics International 39 (2013) 2715–2721

CERAMICS INTERNATIONAL

www.elsevier.com/locate/ceramint

Influence of grain size on high temperature oxidation behavior of Cr_2AlC ceramics

Shibo Li[a,*], Xiaodong Chen[a], Yang Zhou[a], Guiming Song[b]

[a]*Center of Materials Science and Engineering, School of Mechanical and Electronic Control Engineering, Beijing Jiaotong University, Beijing 100044, China*
[b]*Department of Materials Science and Engineering, Delft University of Technology, Mekelweg 2, 2628 CD Delft, The Netherlands*

Received 6 September 2012; received in revised form 12 September 2012; accepted 12 September 2012
Available online 26 September 2012

Abstract

The influence of grain size on the oxidation behavior of Cr_2AlC at 1100 °C and 1200 °C for different times was investigated using fine grained (2 μm) and coarse grained (60 μm) samples. The two materials show a good oxidation resistance owing to the formation of a dense and continuous Al_2O_3 layer. The oxidation rate of the fine grained Cr_2AlC is relatively faster than that of the coarse grained Cr_2AlC. The microstructure and phase composition of scale was characterized. After oxidation at 1100 °C and 1200 °C for long times up to 100 h, only a dense and continuous α-Al_2O_3 oxide layer formed on both the fine grained and coarse grained Cr_2AlC. However, after oxidation at 1100 °C for a relatively short 2 h period, a Cr_7C_3 compound was detected beneath the α-Al_2O_3 oxide layer on the coarse grained Cr_2AlC, yet no Cr_7C_3 was found in the fine grained Cr_2AlC. The oxidation mechanism of the fine and the coarse grained Cr_2AlC was discussed.

Keywords: A. Hot pressing; B. Grain size; C. Corrosion; D. Carbides

1. Introduction

MAX phase materials (M denotes an early transition metal, *A* is a mostly IIIA or IVA group element, and *X* is either *C* or *N*) have been studied extensively because they exhibit unusual, and sometimes unique properties at both room and high temperatures [1–9].

It is well known that properties of materials are strongly dependent on their microstructures. A fine grained microstructure of the MAX phase materials has a strong effect on their mechanical properties [10–15]. For example, a fine grained Ti_3SiC_2 (with a grain size of about 3–5 μm) has a high flexural strength. Its measured strength was 600 MPa, being much higher than 350 MPa for a coarse grained Ti_3SiC_2 (100–200 μm) [10–12]. The flexural strength of a Ti_3AlC_2 ceramic with a grain size of 28 μm in length and 6.5 μm in width was 300 MPa, which is higher than 169 MPa for the coarse one with a grain size of 75 μm in length and 19 μm in width [13]. A fine grained Ti_2SC (2–4 μm) is harder than a coarse grained Ti_2SC (10–20 μm), viz. 8 GPa versus 6 GPa in Vickers hardness [14]. The flexural strength and Vickers hardness of a fine grained Cr_2AlC (2 μm) ceramic were 513 MPa and 6.4 GPa, respectively. These mechanical properties are much higher than those of a coarse grained Cr_2AlC (35 μm) ceramic, viz. 305 MPa and 3.5 GPa, respectively [15]. However, those fine grained MAX phase ceramics are more brittle, less damage tolerant and thermal shock resistant than the coarse grained ceramics [11,14,15].

In addition, the grain size also plays an important role in influencing the wear behavior of the MAX phases. For example, a coarse grained Ti_3SiC_2 (100 μm) showed a better wear resistance in sliding and abrasive wear tests than a fine grained one (5 μm). Multiple energy-dissipating mechanisms including delamination, crack bridging, grain buckling, microcracking, and grain fracture are responsible for the enhanced wear resistance of the coarse grained Ti_3SiC_2 relative to the fine grained Ti_3SiC_2 where only grain pull out and fracture were observed [16]. Furthermore, it was reported that different grain sized Ti_3SiC_2 materials exhibited different creep behaviors in the 1000–1300 °C temperature range [17–19].

*Corresponding author. Tel./fax: +86 10 51685554.
E-mail address: shbli1@bjtu.edu.cn (S. Li).

0272-8842/$ - see front matter © 2012 Elsevier Ltd and Techna Group S.r.l. All rights reserved.
http://dx.doi.org/10.1016/j.ceramint.2012.09.039

Although the influence of the grain size on the above mentioned properties of MAX materials has been carried out, yet so far there has been less information about such an influence on high temperature oxidation behavior of MAX materials. In this work Cr_2AlC was chosen for studying the relationship between grain size and oxidation behavior. In recent years, Cr_2AlC as one of the most attractive materials in the MAX phases has been reported with an enhanced oxidation resistance due to the formation of a dense primarily α-Al_2O_3 containing layer at high temperatures [20–24]. However, there are still arguments on its oxidation behavior, especially on the phase composition in the oxidation layer. For example, Lin et al. [20] investigated the isothermal oxidation behavior of Cr_2AlC (grain size of ~15 μm) at 800–1300 °C in air for 20 h. They found that the oxidation kinetics of Cr_2AlC followed a parabolic rate law, and the formed scale was comprised of a continuous and homogenous outer Al_2O_3-rich layer and a Cr_7C_3 inner layer. Tian et al. [21] performed the isothermal oxidation test of Cr_2AlC (grain size of ~30 μm) at 1100 °C and 1250 °C in air for 20 h and found the similar oxidation behavior and composition in scale as reported by Lin. Lee et al. [22] studied the isothermal oxidation behavior of Cr_2AlC (grain size of ~18 μm) at 900–1200 °C in air for 50 h and reported that the oxidation kinetics of Cr_2AlC did not follow a parabolic rate law at above 1100 °C, and the scale consisted of an outer layer of Al_2O_3 and an inner layer of Cr_7C_3. They further investigated the cyclic oxidation behavior of Cr_2AlC at 1000–1300 °C in air up to 100 h, and found that scales formed at 1000 °C and 1100 °C were comprised of a dense Al_2O_3 outer layer and a Cr_7C_3 inner layer; whereas scales formed at 1200 °C and 1300 °C were comprised of an outer layer containing a mixture of Al_2O_3 and Cr_2O_3 oxides, and an inner layer containing Al_2O_3 and Cr_7C_3 [23]. Recently we found that only a dense and continuous Al_2O_3 scale without the presence of Cr_7C_3 and Cr_2O_3 on a fine grained Cr_2AlC (2 μm) after oxidation at 900–1200 °C for 100 h in air [24].

The above results indicate that the oxidation behavior and the formation of reactants may be dependent on the microstructure and chemical compositions of Cr_2AlC. To support this interpretation, in the present study, fine and coarse grained Cr_2AlC specimens were prepared. The influence of grain size on the oxidation behavior of Cr_2AlC was investigated.

2. Experimental procedures

The fabrication of fine and coarse grained Cr_2AlC samples can be found in elsewhere.[15,25] Briefly, the fine grained Cr_2AlC (denoted as FG Cr_2AlC) with size of 2 μm was prepared by hot pressing a mechanically alloyed mixture of Cr, Al and C with a molar ratio of Cr:Al:C = 2:1.2:1 at 1100 °C for 1 h under 30 MPa in an Ar atmosphere. The coarse grained Cr_2AlC (denoted as CG Cr_2AlC) with size of 60 μm was achieved by hot pressing $AlCr_2$ and C powders with a molar ratio of 1:1 at 1400 °C with 20 MPa for 1 h in Ar. The microstructures of the synthesized samples were identified with scanning electron microscopy (SEM) using a JEOL JSM 6500F field emission gun scanning electron microscope (Tokyo, Japan) equipped with an energy-dispersive X-ray spectrometer (EDS).

The produced samples were cut into bars with dimensions of $10 \times 4 \times 3\ mm^3$. The bars were ground with SiC papers and then polished down to 1 μm using diamond paste, and finally cleaned thoroughly using ultrasonic bath and ethanol.

The isothermal oxidation test was performed at 1100 and 1200 °C for different times in synthetic air (20 vol.% O_2 and 80 vol.% N_2) in a TGA (Setsys Evolution, SETARAM, Caluire, France). The phase compositions of the oxidized samples were characterized by X-ray diffraction (XRD) analysis with a D/Max 2200 PC diffractometer (Tokyo, Japan) using Cu K_α radiation.

The oxidized samples were polished using a JEOL SM09010 cross section ion polisher (Tokyo, Japan) for cross-sectional observation with SEM. The chemical composition of the scale was analyzed with electron probe micro analysis (EPMA) with a JEOL JXA 8900R microprobe (Tokyo, Japan) using an electron beam with energy of 10 keV and beam current of 200 nA employing wavelength dispersive spectrometry (WDS).

3. Results

The microstructures of the FG and CG Cr_2AlC are demonstrated in Fig. 1. The average grain sizes of the FG and CG Cr_2AlC are 2 μm and 60 μm, respectively. The synthesized FG and CG Cr_2AlC samples have a high density of 99%, with a small amount of Al_2O_3 as an impurity [15,25].

Fig. 2 shows the oxidation behaviors of the two Cr_2AlC materials. The oxidation rates at 1100 °C for both materials are slow, but become relatively fast as temperature increases to 1200 °C. For the FG Cr_2AlC samples, the weight gain increases from $0.69 \times 10^{-2}\ kg/m^2$ at 1100 °C to $1.78 \times 10^{-2}\ kg/m^2$ at 1200 °C for 100 h. However, for their CG counterparts, the weight gain increases from $0.47 \times 10^{-2}\ kg/m^2$ at 1100 °C to $1.54 \times 10^{-2}\ kg/m^2$ at 1200 °C for 100 h. The above results indicate that the oxidation rate of the FG Cr_2AlC is relatively faster than that of the CG Cr_2AlC both at 1100 °C and 1200 °C, probably due to the fact that the FG Cr_2AlC provides faster grain-boundary diffusion paths than CG Cr_2AlC.

Fig. 3 shows the oxidation kinetics of the FG and the CG Cr_2AlC. The relationships between square of mass gain per unit surface area and oxidation time at 1100 °C and 1200 °C for the FG Cr_2AlC are not linear (Fig. 3(a)), indicating that the oxidation kinetics of FG Cr_2AlC does not follow a parabolic rate law. For comparison, cube of mass gain per unit surface area of FG Cr_2AlC as a function of oxidation time was also demonstrated; see Fig. 3(b). It was found that the 1100 °C-curve deviated

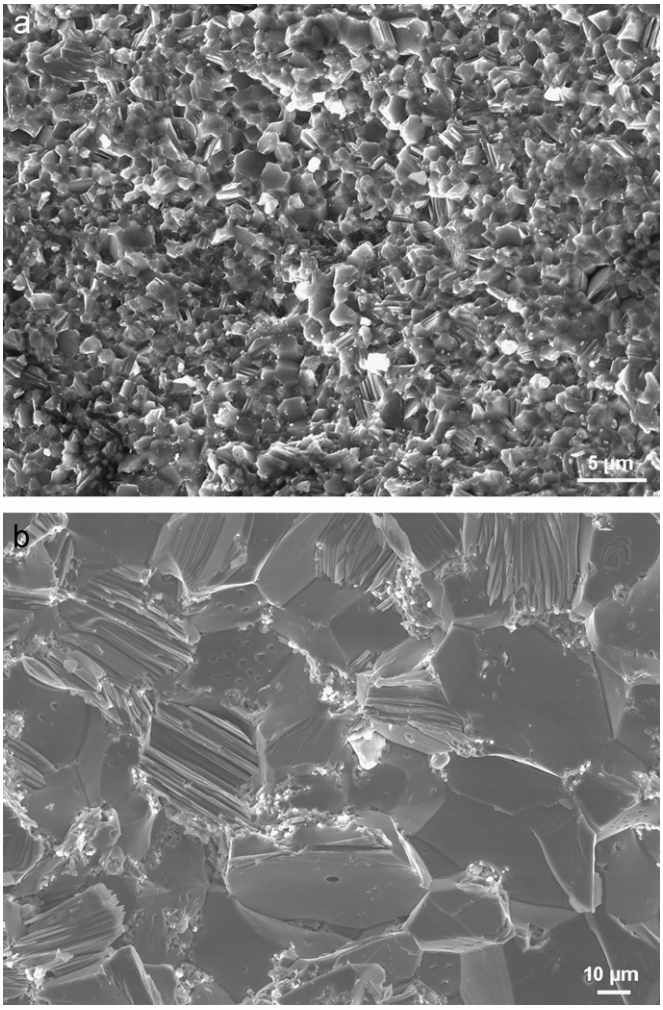

Fig. 1. SEM micrographs of (a) fine and (b) coarse grained Cr_2AlC.

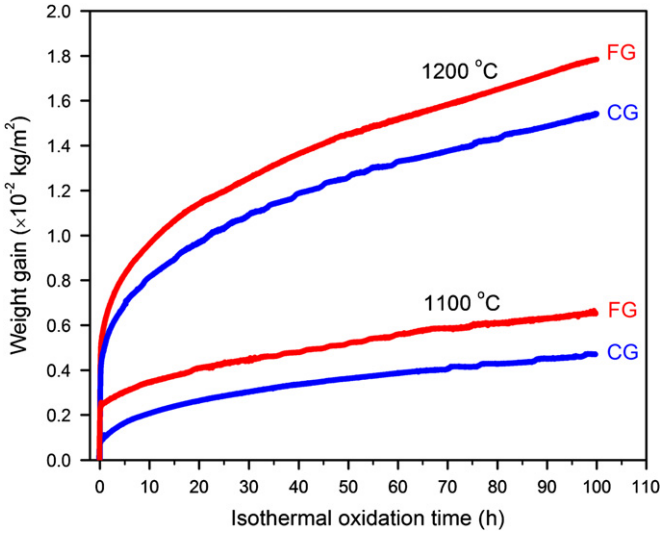

Fig. 2. Oxidation behaviors of fine (FG) and coarse grained (CG) Cr_2AlC ceramics at 1100 °C and 1200 °C for 100 h.

from a cubic rate law (Inset in Fig. 3(b)), yet the 1200 °C-curve roughly followed a cubic rate law (Fig. 3(b)). The above results indicate that the oxidation kinetics for the FG Cr_2AlC is much complex, which follows neither the parabolic rate law nor the cubic law at 1100 °C for 100 h, but approximately abides by a cubic rate law at 1200 °C for 100 h. However, the oxidation kinetics of the CG Cr_2AlC followed a cubic rate law at 1100 °C and 1200 °C for 100 h (Fig. 3(c)).

After oxidation at 1100 °C and 1200 °C for 100 h, only a continuous and dense Al_2O_3 scale was found on the FG and the CG samples. Fig. 4 shows typical cross-sectional SEM images of the FG and the CG samples after isothermal oxidation at 1100 °C for 100 h. The average thickness of the Al_2O_3 scale on the FG Cr_2AlC is about 3 μm (Fig. 4 (a)), and about 2 μm on the CG Cr_2AlC (Fig. 4(b)). It is worth noting that neither binary carbides nor Cr_2O_3 is detected in the scale after oxidation at both 1100 °C and 1200 °C for 100 h. The EPMA result (Fig. 5) shows that the oxide scale on FG Cr_2AlC is composed of Al and O elements, corresponding to Al_2O_3. XRD results further proved that only α-Al_2O_3 as a new phase was detected in the FG and CG Cr_2AlC samples after oxidation at 1100 °C and 1200 °C for 100 h.

In the present study, no Cr_7C_3 or other Cr–C phases as oxidative products was found after oxidation at high temperatures up to 100 h. It is anticipated that the Cr–C phases might form at an early oxidation stage and then were oxidized after oxidation for a certain time. In order to support this interpretation, the isothermal oxidation tests for the FG and CG Cr_2AlC samples at 1100 °C and 1200 °C for 2 h were performed.

After oxidation at 1100 °C for 2 h, there was only a dense Al_2O_3 scale on the FG Cr_2AlC (Fig. 6(a)). However, it was found some Cr_7C_3 (confirmed by EDS and XRD) beneath the Al_2O_3 layer on the CG Cr_2AlC (Fig. 6(b)). Fig. 7 shows the phase compositions of the above oxidized samples. The diffractogram of the FG samples after oxidation at 1100 °C for 2 h shows peaks belonging to α-Al_2O_3 and Cr_2AlC (Fig. 7(a)). The diffractogram of the CG samples after oxidation at 1100 °C for 2 h shows peaks corresponding to the following three phases: Cr_2AlC, α-Al_2O_3 and Cr_7C_3 (Fig. 7(b)). Peaks corresponding to Cr_2AlC were still detectable in the XRD patterns, suggesting that the oxidation layers formed on the FG and CG Cr_2AlC are thin.

4. Discussion

According to the above results, the oxidation mechanism for the Cr_2AlC ceramics is discussed as follows:

The hexagonal crystal structure of Cr_2AlC consists of CrC_6 octahedra linked by Al atom layers. The bond between CrC_6 and the Al layer is weak, so Al atoms diffuses easily from Cr_2AlC and selective oxidation of Al into α-Al_2O_3 takes places as described in reactions (1) and (2). The theoretical work predicted that the Al-containing Ti_2AlC with a high (up to 50%) vacancy concentration on the Al lattice still sustain its phase stability and keep its structural integrity [26]. The crystal structure of Cr_2AlC is

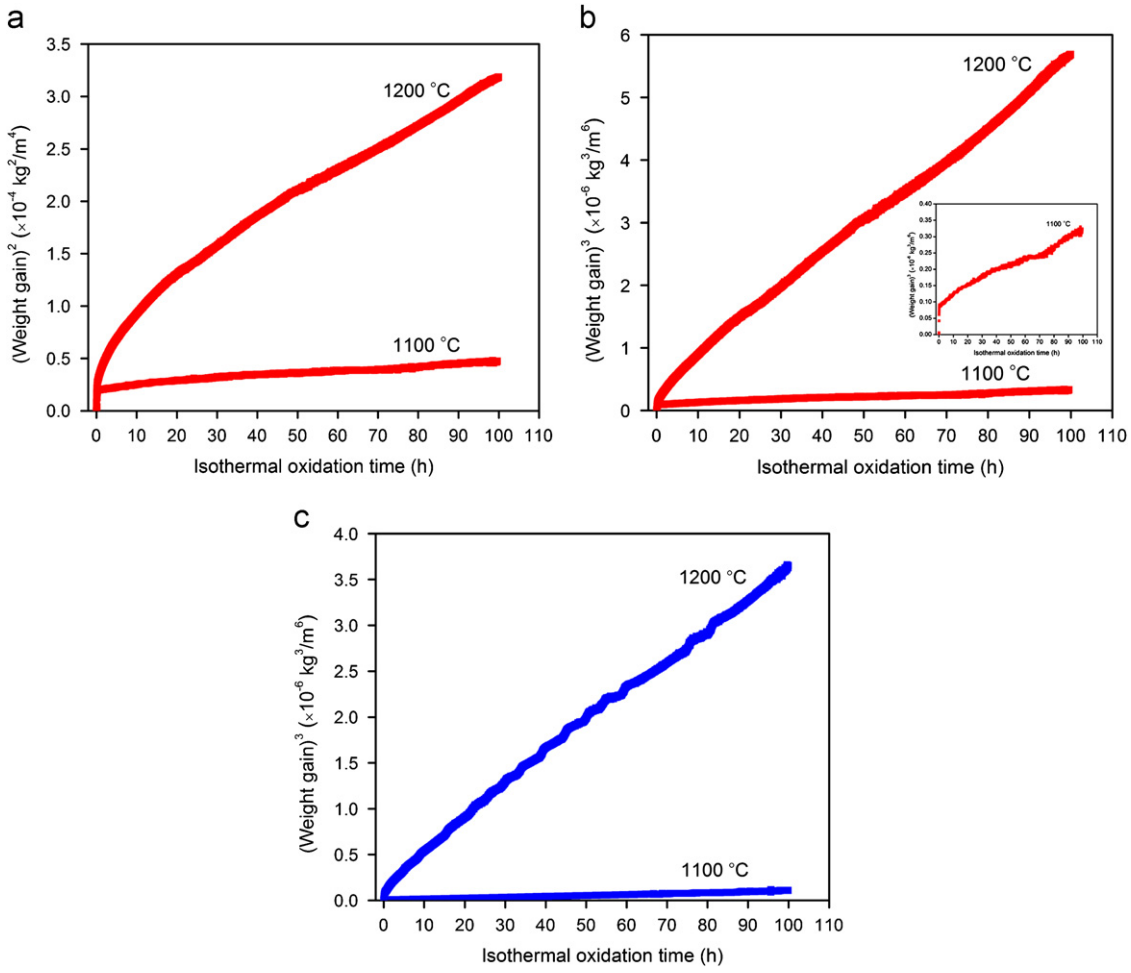

Fig. 3. Oxidation kinetics of FG and CG Cr_2AlC at 1100 °C and 1200 °C for 100 h. (a) parabolic plot for FG Cr_2AlC. (b) cubic plot for FG Cr_2AlC. Inset in (b) showing an enlarged 1100 °C curve. (c) cubic plot for CG Cr_2AlC.

similar to that of Ti_2AlC. So it is reasonable to speculate that Al-depleted $Cr_2Al_{1-x}C$ still keeps the same crystal structure as Cr_2AlC even x is up to 0.5.

$$Cr_2AlC \rightarrow Cr_2Al_{1-x}C + xAl \ (x=0\text{–}0.5) \quad (1)$$

$$Al + 3O = Al_2O_3 \quad (2)$$

It is well known the finer the grains, the larger the area of grain boundaries in bulk materials. Grain boundaries provide a rapid diffusion path. Hence the outward diffusion of Al in the FG Cr_2AlC is much quickly as compared to the CG Cr_2AlC. The FG Cr_2AlC acts as a ''reservoir'' for supplying sufficient Al through the rapid diffusion path to form Al_2O_3 on surface. Hence a thin protective Al_2O_3 film forms rapidly on the FG sample. The formation of the Al_2O_3 film will retard both the rapid outward diffusion of Al and inward diffusion of O. Therefore, the Al_2O_3 scale grows very slowly (viz. only ~3 μm after oxidation at 1100 °C for 100 h.) on the FG Cr_2AlC. In this case, $Cr_2Al_{1-x}C$ is stable without decomposition into Cr–C binary carbides (such as Cr_7C_3 and Cr_3C_2). This is the reason why no Cr–C carbides formed on the FG Cr_2AlC after oxidation at 1100 °C even for a short time of 2 h. The above mechanism has also been addressed by the previous research on the oxidation of Ti_2AlC [27–30]. In addition, Wang et al. [31] investigated the oxidation mechanism of Ti_3AlC_2 and reported that the Al element diffused from Ti_3AlC_2 so fast and the selective oxidation of Al occurred according to $Ti_3AlC_2 + 3/2\ O_2 = Ti_3Al_{1-y}C_2 + 1/2yAl_2O_3$. The fast diffusion and selective oxidation of Al resulted in a protective Al_2O_3 scale, rather than a mixed TiO_2 and Al_2O_3 layer, on Ti_3AlC_2 with Al vacancy substrate.

Herein, we do not exclude another possibility that Cr–C carbides may form in the FG Cr_2AlC before 2 h during oxidation at 1100 °C. If the depletion of Al near surface zones is severe, which might cause the decomposition of part of Cr_2AlC into Cr_2C as described in reaction (3). The Cr_2C phase is then oxidized with the formation of Cr_7C_3, Cr_2O_3, and CO or CO_2 (for brevity, only noted as CO_2) according to reaction (4). The Cr_7C_3 phase is finally oxidized according to reaction (5). In the present study, no Cr_2O_3 was found in the scales formed at 1100 °C and 1200 °C, owing to the evaporation of Cr_2O_3 at above 1100 °C [32].

$$Cr_2Al_{1-x}C \rightarrow Cr_2C + xAl \ (x > 0.5) \quad (3)$$

$$9Cr_2C + 12O_2 = 2Cr_7C_3 + 9CO_2\uparrow + 2Cr_2O_3\uparrow \quad (4)$$

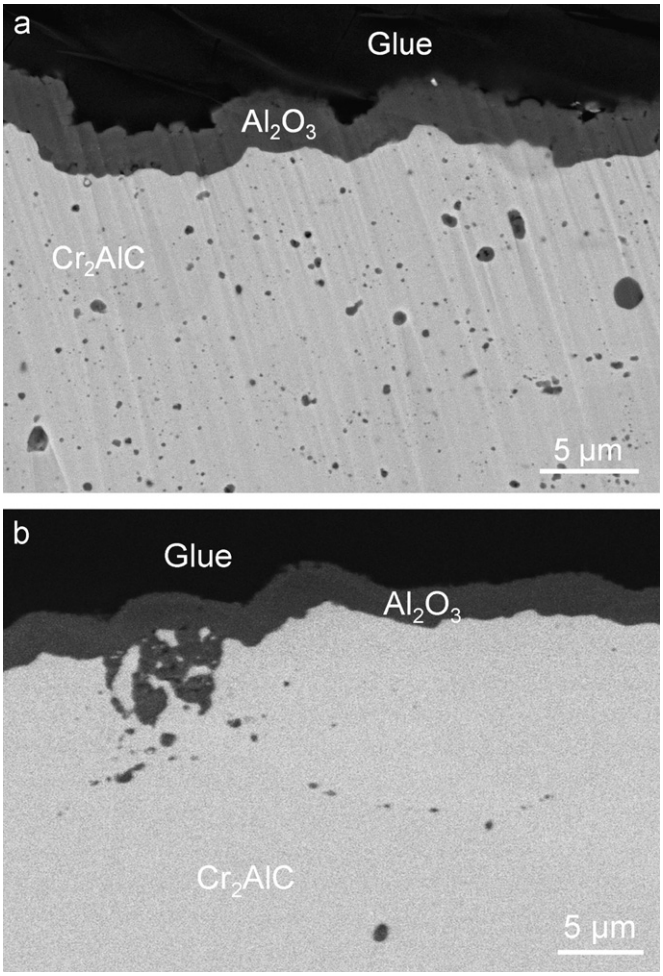

Fig. 4. Backscattered electron cross-sectional images of (a) fine and (b) coarse grained Cr_2AlC after isothermal oxidation at 1100 °C for 100 h. The black particles in the Cr_2AlC matrix are Al_2O_3 impurity from the synthesized samples.

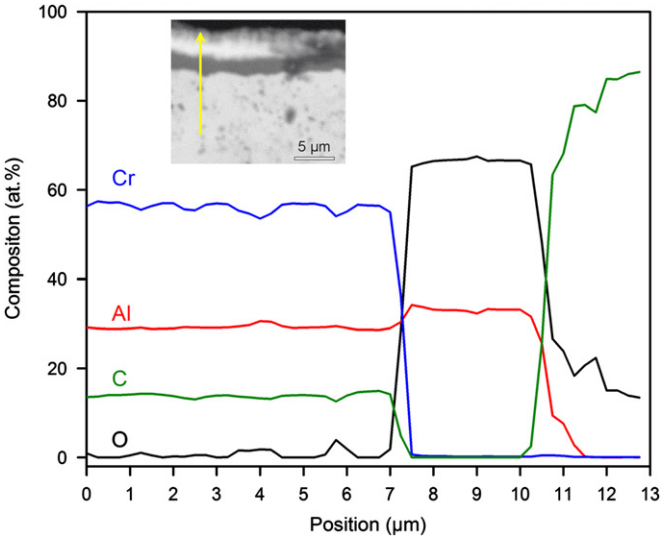

Fig. 5. EPMA result for the composition along a straight line (shown in the inset) in the fine grained Cr_2AlC after oxidation at 1100 °C for 100 h.

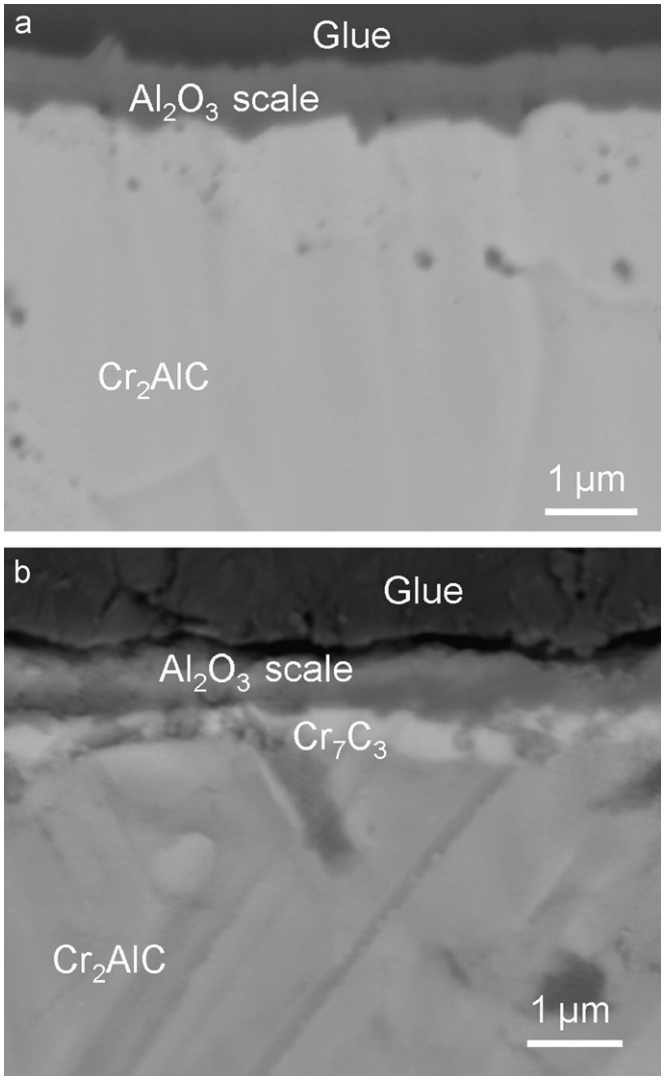

Fig. 6. Backscattered electron cross-sectional images of (a) fine and (b) coarse grained Cr_2AlC after isothermal oxidation at 1100 °C for 2 h.

$$2Cr_7C_3 + 16.5O_2 = 7Cr_2O_3\uparrow + 6CO_2\uparrow \quad (5)$$

The reactions (3–5) may occur quickly at an early oxidation stage (before a continuous and dense α-Al_2O_3 scale is formed), because no Cr_7C_3 was found in the FG Cr_2AlC after oxidation at 1100 °C for 2 h. After a continuous Al_2O_3 film forms with a certain thickness, reactions (1) and (2) predominate again. From the above discussion, it may explain the reason why only the Al_2O_3 scale develops on the FG Cr_2AlC.

For CG Cr_2AlC, the oxidation process also follows the sequence of reactions (1) and (2). However, the outward diffusion rate of Al through the whole CG Cr_2AlC to the surface is relatively slow, because there is less amounts of grain boundaries in the CG Cr_2AlC as compared with the FG Cr_2AlC. Hence the time for the formation of a continuous Al_2O_3 protective layer on the CG Cr_2AlC may be prolonged. Without the continuous Al_2O_3 covering layer, the depletion of Al near the surface is severe,

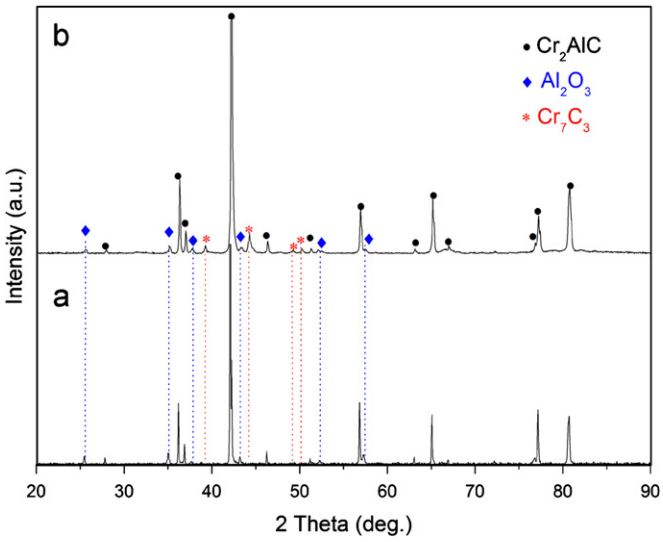

Fig. 7. XRD patterns of (a) fine and (b) coarse grained Cr_2AlC after isothermal oxidation at 1100 °C for 2 h.

resulting in the decomposition of $Cr_2Al_{1-x}C$ into Cr_2C. The oxidation of Cr_2C makes the formation of Cr_7C_3 as described in reactions (3) and (4). Once a continuous Al_2O_3 layer with a certain thickness forms with increasing time, the thermal decomposition of Cr_2AlC may stop and no new Cr–C compounds forms further. Consequently, the previously formed Cr_7C_3 and Cr_2C compounds will be oxidized gradually. Finally a dense Al_2O_3 scale forms on the CG sample as shown in Fig. 4(b). This maybe explains the reason why Cr_7C_3 was detected beneath the Al_2O_3 layer on the CG Cr_2AlC after oxidation for 2 h and then disappeared completely for long times up to 100 h.

5. Conclusions

The influence of grain sizes on oxidation behavior of Cr_2AlC was investigated. Based on the above analysis, the main conclusions are as follows:

The isothermal oxidation at 1100 °C and 1200 °C for times up to 100 h shows that the fine grained (2 μm) and the coarse grained (60 μm) Cr_2AlC possess a good oxidation resistance owing to the formation of a dense and continuous Al_2O_3 scale, which prevents the materials from further oxidation.

The oxidation rate of the fine grained Cr_2AlC samples is faster than that of the coarse grained samples, due to that the former provides a large amount of grain boundaries. For the fine grained Cr_2AlC samples, the weight gain increases from 0.69×10^{-2} kg/m^2 at 1100 °C to 1.78×10^{-2} kg/m^2 at 1200 °C for 100 h. However, for the coarse grained Cr_2AlC, the weight gain increases from 0.47×10^{-2} kg/m^2 at 1100 °C to 1.54×10^{-2} kg/m^2 at 1200 °C for 100 h.

Some Cr_7C_3 were found beneath the α-Al_2O_3 layer on the coarse grained Cr_2AlC, whereas no such compound was detected in the fine grained Cr_2AlC after oxidation at 1100 °C for 2 h. After oxidation at 1100 °C and 1200 °C for times up to 100 h, only an α-Al_2O_3 scale was found on both the fine and the coarse grained Cr_2AlC.

Acknowledgments

This work was supported by the National Natural Science Foundation of China under Grant nos. 51072017, 50972006 and 51172015, and "Hongguoyuan" Talent Foundation of Beijing Jiaotong University, and The Delft Center of Materials Research Program on Self Healing Materials, and the Dutch IOP program on Self Healing Materials under Grant no. IOP-SHM 0871.

References

[1] M.W. Barsoum, The $M_{n+1}AX_n$ phases: a new class of solids; thermodynamically stable nanolaminates, Progress in Solid State Chemistry 28 (2000) 201–281.
[2] H.B. Zhang, Y.W. Bao, Y.C. Zhou, Current Status in layered ternary Carbide Ti_3SiC_2, a review, Journal of Materials Science and Technology 25 (2009) 1–38.
[3] M.W. Barsoum, M. Radovic, Elastic and mechanical properties of the MAX phases, Annual Review of Materials Research 41 (2011) 195–227.
[4] X.H. Wang, Y.C. Zhou, Layered machinable and electrically conductive Ti_2AlC and Ti_3AlC_2 ceramics: a review, Journal of Materials Science and Technology 26 (2010) 385–416.
[5] Z.M. Sun, Progress in research and development on MAX phases: a family of layered ternary compounds, International Materials Reviews 56 (2011) 143–166.
[6] J.Y. Wang, Y.C. Zhou, Recent progress in theoretical prediction, preparation, and characterization of layered ternary transition-metal carbides, Annual Review of Materials Research 39 (2009) 10.1–10.29.
[7] P. Eklund, M. Beckers, U. Jansson, H. Högberg, L. Hultman, The $M_{n+1}AX_n$ phases: materials science and thin-film processing, Thin Solid Films 518 (2010) 1851–1878.
[8] S.B. Li, G.M. Song, C. Kwakernaak, S. van der Zwaag, W.G. Sloof, Multiple crack healing of a Ti_2AlC ceramic, Journal of the European Ceramic Society 32 (2012) 1813–1820.
[9] G.M. Song, S.B. Li, C.X. Zhao, W.G. Sloof, S. van der Zwaag, Y.T. Pei, J.Th.M. de Hosson, Ultra-high temperature ablation of Ti_2AlC ceramics under an oxyacetylene flame, Journal of the European Ceramic Society 31 (2011) 855–862.
[10] M. Radovic, M.W. Barsoum, T. El-Raghy, S.M. Wiederhorn, W.E. Luecke, Effect of temperature, strain rate and grain size on the mechanical response of Ti_3SiC_2 in tension, Acta Materialia 50 (2002) 1297–1306.
[11] T. El-Raghy, M.W. Barsoum, A. Zavaliangos, S.R. Kalidindi, Processing and mechanical properties of Ti_3SiC_2. II. Effect of grain size and deformation temperature, Journal of the American Ceramic Society 82 (1999) 2855–2860.
[12] C.J. Gilbert, D.R. Bloyer, M.W. Barsoum, T. El-Raghy, A.P. Tomsia, R.O. Ritchie, Fatigue-crack growth and fracture properties of coarse and fine-grained Ti_3SiC_2, Scripta Materialia 238 (2000) 761–767.
[13] D.T. Wan, F.L. Meng, Y.C. Zhou, Y.W. Bao, J.X. Chen, Effect of grain size, notch width, and testing temperature on the fracture toughness of $Ti_3Si(Al)C_2$ and Ti_3AlC_2 using the chevron-notched beam (CNB) method, Journal of the European Ceramic Society 28 (2008) 663–669.
[14] S. Amini, M.W. Barsoum, T. El-Raghy, Synthesis and mechanical properties of fully dense Ti_2SC, Journal of the American Ceramic Society 90 (2007) 3953–3958.
[15] S.B. Li, W.B. Yu, H.X. Zhai, G.M. Song, W.G. Sloof, S. van der Zwaag, Mechanical properties of low temperature synthesized dense and fine grained Cr_2AlC ceramics, Journal of the European Ceramic Society 31 (2011) 217–224.

[16] T. El-Raghy, P. Blau, M.W. Barsoum, Effect of grain size on friction and wear behavior of Ti_3SiC_2, Wear 238 (2000) 125–130.
[17] M. Radovic, M.W. Barsoum, T. El-Raghy, S.M. Wiederhorn, Tensile creep of coarse-grained (100–300 μm) Ti_3SiC_2 in the 1000–1200 °C temperature range, Journal of Alloys and Compounds 361 (2003) 299–312.
[18] M. Radovic, M.W. Barsoum, T. El-Raghy, S.M. Wiederhorn, Tensile creep of fine-grained (3–5 μm) Ti_3SiC_2 in the 1000–1200 °C temperature range, Acta Materialia 49 (2001) 4103–4112.
[19] T. Zhen, M.W. Barsoum, S.R. Kalidindi, M. Radovic, Z.M. Sun, T. El-Raghy, Compressive creep of fine and coarse-grained Ti_3SiC_2 in air in the 1000–1200 °C temperature range, Acta Materialia 53 (2005) 4963–4973.
[20] Z.J. Lin, M.S. Li, J.Y. Wang, Y.C. Zhou, High-temperature oxidation and hot corrosion of Cr_2AlC, Acta Materialia 55 (2007) 6182–6191.
[21] W.B. Tian, P.L. Wang, Y.M. Kan, G.J. Zhang, Oxidation behavior of Cr_2AlC ceramics at 1100 and 1250 °C, Journal of Materials Science 43 (2008) 2785–2791.
[22] D.B. Lee, S.W. Park, Oxidation of Cr_2AlC between 900 and 1200 °C in air, Oxidation of Metals 68 (2007) 211–222.
[23] D.B. Lee, T.D. Nguyen, Cyclic oxidation of Cr_2AlC between 1000 and 1300 °C in air, Journal of Alloys and Compounds 466 (2008) 434–439.
[24] S.B. Li, L.O. Xiao, G.M. Song, W.G. Sloof, S. van der Zwaag, Oxidation and self-healing behavior of a fine-grained Cr_2AlC ceramic, Submitted for publication.
[25] L.O. Xiao, S.B. Li, G.M. Song, W.G. Sloof, Synthesis and thermal stability of Cr_2AlC, Journal of the European Ceramic Society 31 (2011) 1497–1502.
[26] J.Y. Wang, Y.C. Zhou, T. Liao, J. Zhang, Z.J. Lin, A first-principles investigation of the phase stability of Ti_2AlC with Al vacancies, Scripta Materialia 58 (2008) 227–230.
[27] X.H. Wang, Y.C. Zhou, High-temperature oxidation behavior of Ti_2AlC in air, Oxidation of Metals 59 (2003) 303–320.
[28] H.J. Yang, Y.T. Pei, J.C. Rao, J.ThM. de Hosson, S.B. Li, G.M. Song, High temperature healing of Ti_2AlC: on the origin of inhomogeneous oxide scale, Scripta Materialia 65 (2011) 135–138.
[29] G.M. Song, V. Schnabel, C. Kwakernaak, S. van der Zwaag, J.M. Schneider, W.G. Sloof, High temperature oxidation behavior of Ti_2AlC ceramic at 1200 °C, Materials at High Temperatures 29 (2012) 205–209.
[30] S.B. Li, G.M. Song, K. Kwakernaak, S. van der Zwaag, W.G. Sloof, Multiple crack healing of a Ti_2AlC ceramic, Journal of the European Ceramic Society 32 (2012) 1813–1820.
[31] X.H. Wang, F.Z. Li, J.X. Chen, Y.C. Zhou, Insight into high temperature oxidation of Al_2O_3-forming Ti_3AlC_2, Corrosion Science 58 (2012) 95–103.
[32] M.P. Brady, P.F. Tortorelli, Alloy design of intermetallics for protective scale formation and for use as precursors for complex ceramic phase surfaces, Intermetallics 12 (2004) 779–789.